Inorg. Chem. **2008**, *47*, 3371−3378

Water Substitution on Iron Centers: from 0D to 1D Sandwich Type Polyoxotungstates

Anne Dolbecq,* Jean-Daniel Compain, Pierre Mialane, Jérôme Marrot, Eric Rivière, and Francis Sécheresse

Institut Lavoisier, IREM, UMR 8180, Université de Versailles Saint-Quentin en Yvelines, 45 Avenue des Etats-Unis, 78035 Versailles Cedex, France

Received December 14, 2007

Four novel polyoxotungstates have been synthesized by reaction of the sandwich type compound $[Fe^{III}_4(H_2O)_{10}(B\text{-}\beta\text{-}SbW_9O_{33})_2]^{6-}$ (noted $Fe_4(H_2O)_{10}Sb_2W_{18}$) with ethylenediamine (en) and/or oxalate (ox) ligands under various conditions. The one-dimensional (1D) compound $[enH_2]_3[Fe^{III}_4(H_2O)_8(SbW_9O_{33})_2]\cdot 20H_2O$ (**1**) is isolated at 130 °C and results from the elimination of two water molecules and the condensation of the polyoxotungstate precursor. The reaction of $Fe_4(H_2O)_{10}Sb_2W_{18}$ with oxalate ligands affords the molecular complex $Na_{14}[Fe^{III}_4(ox)_4(H_2O)_2(SbW_9O_{33})_2]\cdot 60H_2O$ (**2**) where two organic ligands substitute four water molecules, while the same reaction in the presence of en molecules at 130 °C leads to the formation of the functionalized 1D chain $[enH_2]_7[Fe^{III}_4(ox)_4(SbW_9O_{33})_2]\cdot 14H_2O$ (**3**) with protonated ethylenediamine counterions. Finally, at 160 °C a rearrangement of the $Fe_4(H_2O)_{10}Sb_2W_{18}$ polyoxotungstate is observed, and the sandwich type compound $[enH_2]_5[Fe^{II}_2Fe^{II}_2(enH)_2(Fe^{III}W_9O_{34})_2]\cdot 24H_2O$ (**4**) crystallizes. In **4**, the heteroelement is a Fe^{III} ion, and the water molecules on the two outer Fe^{II} centers are bound to pendant monoprotonated en ligands. The four compounds have been characterized by IR spectroscopy, thermogravimetric analysis, and single crystal X-ray diffraction. A detailed study of the magnetic properties of the mixed-valent hexanuclear iron complex in **4** shows evidence of an $S = 5$ ground-state because of spin frustration effects. A quantification of the electronic parameters characterizing the ground state ($D = +1.12$ cm^{-1}, $E/D = 0.15$) confirms that polyoxotungstate ligands induce large magnetic anisotropy.

Introduction

The structure of the Keggin type polyoxometalate (POM) $\{XM_{12}O_{40}\}$ has been known for more than seven decades, and this anion remains probably the best known and most studied POM. It still raises interest because of its potential applications in the fields of catalysis, medicine, and material chemistry.[1] While the properties of Keggin complexes have been mostly studied for X = P^V, Si^{IV} and M = W, Mo, this structural type has been characterized with various heteroatoms and metal oxide fragments and even one with a Mn^{II} ion trapped at the center of a cage of twelve SbO_6 octahedra has been encountered.[2] Removal of three W atoms of the Keggin anion leads to highly charged trivacant species able to act as bulky polydentate ligands toward transition metal ions, leading to a growing family of transition metal substituted POMs. Two categories can be distinguished:[3] (i) the $[XW_9O_{33}]^{n-}$ anions (X = As^{III}, Sb^{III}, Bi^{III}, Se^{IV}), where the heteroelement is pyramidal with a lone electron pair, possess two isomers B-α and B-β and can be described as the association of three $\{W_3O_{13}\}$ groups around the $\{XO_3\}$ central pyramid, and (ii) the $[XW_9O_{34}]^{n'-}$ anions (X = Si^{IV}, Ge^{IV}, P^V, As^V) with a tetrahedral heteroelement possess four isomers, A-α, A-β, B-α, B-β, with the A type corresponding to the association of one $\{W_3O_{13}\}$ group and three $\{W_2O_{10}\}$ groups around the central $\{XO_4\}$ tetrahedron. In the [B-α-$XW_9O_{33}]^{n-}$ (X = As^{III}, Sb^{III}, Bi^{III}, Se^{IV}) anions, the lone pair is directed toward the outside of the open face of the trivacant anion and prevents the formation of complete Keggin type compounds.

Two types of dimeric compounds have been described as the result of the interaction of first row transition metal ions with the $\{XW_9O_{33}\}$ fragment. In the sandwich type $[M_3(H_2O)_3$-

* To whom correspondence should be addressed. E-mail: dolbecq@chimie.uvsq.fr.

(1) Special issue on POMs, *Chem. Rev.* **1998**, *98*, 1.

(2) Baskar, V.; Shanmugam, M.; Helliwell, M.; Teat, S. J.; Winpenny, R. E. P. *J. Am. Chem. Soc.* **2007**, *129*, 3042.

(3) Contant, R.; Hervé, G. *Rev. Inorg. Chem.* **2002**, *22*, 63.

10.1021/ic7024186 CCC: $40.75
Published on Web 02/27/2008

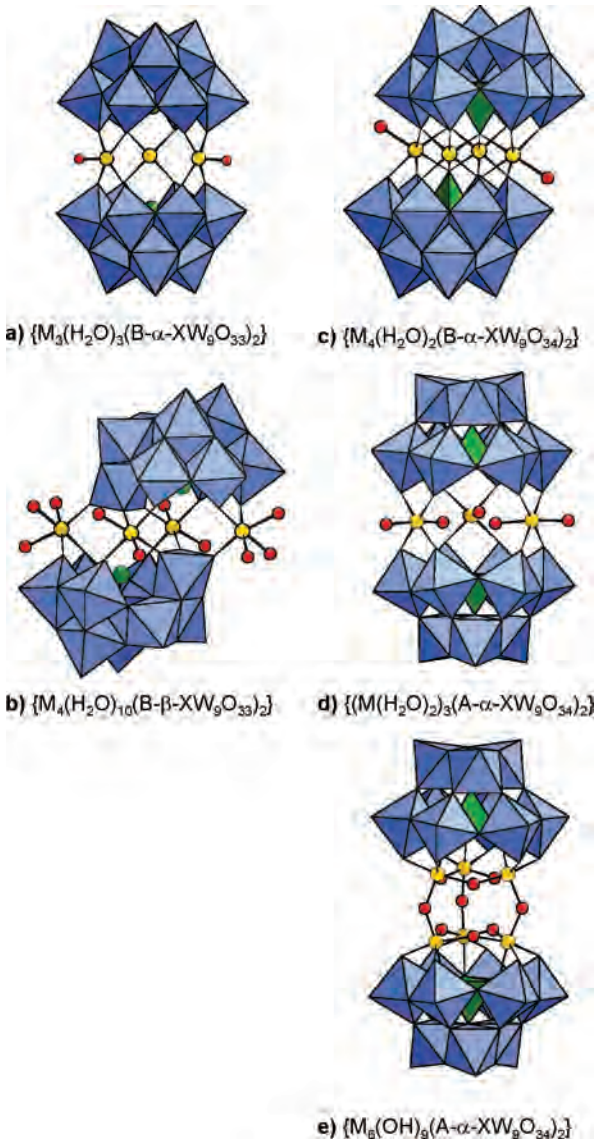

Figure 1. Main structural types of dimeric anions built from trivacant POMs and first row transition metal cations; blue octahedra, WO_6; green spheres, X; green tetrahedra, XO_4; yellow spheres, M; red spheres, O.

$(B\text{-}\alpha\text{-}XW_9O_{33})_2]^{12-}$ anions (Figure 1a), two B-α-XW_9 units are linked by three metal cations.[4] It should be noted that more than three transition metal ions have been incorporated in these sandwich type POMs. The first example described in the literature is the $[Cu_4K_2(H_2O)_8(B\text{-}\alpha\text{-}AsW_9O_{33})_2]^{8-}$ anion.[5a] The Cu_6 and Mn_6 sandwich POMs $[(CuCl)_6(B\text{-}\alpha\text{-}AsW_9O_{33})_2]^{12-}$ and $[(MnCl)_6(B\text{-}\alpha\text{-}SbW_9O_{33})_2]^{12-}$ have also been recently isolated as $[n\text{-}BuNH_3]^+$ salts.[5b] Besides, Krebs et al.[4b] have reported the dimeric $[M_4(H_2O)_{10}(B\text{-}\beta\text{-}XW_9O_{33})_2]^{n-}$ ($X = Te^{IV}$, $M = Mn^{II}$, $n = 8$) anions (Figure 1b). More recently, the analogous compound with $X = Sb^{III}$ and $M = Fe^{III}$ ($n = 6$), noted $Fe_4(H_2O)_{10}Sb_2W_{18}$, has been synthesized by Kortz et al.[6] The structure of this complex consists in two B-β-XW_9 moieties linked by four Fe^{III} ions in an octahedral environment. There are no direct connections between the FeO_6 octahedra, which can be divided in two pairs: in the inner pair the metal centers have two terminal water ligands while in the outer pair the two metal ions have three terminal water ligands. These dimeric anions are also known with two tungsten atoms and two transition metal cations linking the B-β-XW_9 moieties.[7]

The synthesis of dimeric species, considering now the $[XW_9O_{34}]^{n-}$ ligand, depends not only on the isomer (A or B) but also on the nature of the counter-ions (for example Na^+ or K^+) and the pH of the solution, as discussed by Contant and Hervé.[3] Tetranuclear sandwich type complexes $\{M_4(H_2O)_2(B\text{-}\alpha\text{-}XW_9O_{34})_2\}$ (Figure 1c) have been isolated with numerous metals of the first transition row.[8] Different dimeric structures have been obtained with the A-α isomer. In the sandwich type $[(Fe^{III}(H_2O)_2)_3(A\text{-}\alpha\text{-}PW_9O_{34})_2]^{9-}$ POM (Figure 1d) synthesized by Hill et al.[9] and in the copper complex encapsulating a NO_3^- anion,[10] the three metal ions are not directly bound via oxo or hydroxo ligands while in $[Fe_6(OH)_3(A\text{-}\alpha\text{-}GeW_9O_{34}(OH)_3)_2]^{11-}$ (Figure 1e) the Keggin moieties are linked via a trigonal prismatic $Fe_6(OH)_9$ fragment.[11] This type of double sandwich structure with first row transition metal ions has been first structurally characterized for the chromium derivative.[12]

These transition metal substituted anions have been mainly studied for their magnetic[13] and catalytic properties.[14] Up to very recently their syntheses were performed under conventional conditions, that is, at atmospheric pressure and temperatures below 100 °C, but the study of the reactivity of the trivacant XW_9 anions under hydrothermal conditions attracts an increasing interest and has led to the synthesis of novel molecular architectures,[15] one-dimensional (1D)[15b] and

(4) (a) Robert, F.; Leyrie, M.; Hervé, G. *Acta Crystallogr.* **1982**, *B38*, 358. (b) Bösing, M.; Nöb, A.; Loose, I.; Krebs, B. *J. Am. Chem. Soc.* **1998**, *120*, 7252. (c) Mialane, P.; Marrot, J.; Rivière, E.; Nebout, J.; Hervé, G. *Inorg. Chem.* **2001**, *40*, 44. (d) Kortz, U.; Al-Kassem, N. K.; Savelieff, M. G.; Al Kadi, N. A.; Sadakane, M. *Inorg. Chem.* **2001**, *40*, 4742.

(5) (a) Kortz, U.; Nellutla, S.; Stowe, A. C.; Dalal, N. S.; van Tol, J.; Bassil, B. S. *Inorg. Chem.* **2004**, *43*, 144. (b) Yamase, T.; Fukaya, K.; Nojiri, H.; Ohshima, Y. *Inorg. Chem.* **2006**, *45*, 7698.

(6) Kortz, U.; Savelieff, M. G.; Bassil, B. S.; Keita, B.; Nadjo, L. *Inorg. Chem.* **2002**, *41*, 783.

(7) (a) Michelon, M.; Hervé, G. *C. R. Acad. Sci., Ser. C* **1972**, *274*, 209. (b) Loose, I.; Droste, E.; Bösing, M.; Pohlmann, H.; Dickmann, M. H.; Rosu, C.; Pope, M. T.; Krebs, B. *Inorg. Chem.* **1999**, *38*, 2688.

(8) (a) Finke, R. G.; Droege, M.; Huchinson, J. R.; Gansow, O. *J. Am. Chem. Soc.* **1981**, *103*, 1587. (b) Weakley, T. J. R.; Finke, R. G. *Inorg. Chem.* **1990**, *29*, 1235. (c) Gómez-García, C. J.; Coronado, E.; Gómez-Romero, P.; Casañ-Pastor, N. *Inorg. Chem.* **1993**, *32*, 3378. (d) Zhang, X.-Y.; Jameson, G. B.; O'Connor, C. J.; Pope, M. T. *Polyhedron* **1996**, *15*, 917. (e) Zhang, X.; Chen., Q.; Duncan, D. C.; Lachicotte, R. J.; Hill, C. *Inorg. Chem.* **1997**, *36*, 4381. (f) Kortz, U.; Nellutla, S.; Stowe, A. C.; Dalal, N. S.; Rauwald, U.; Danquah, W.; Ravot, D. *Inorg. Chem.* **2004**, *43*, 2308.

(9) Okun, N. M.; Anderson, T. M.; Hill, C. *J. Am. Chem. Soc.* **2003**, *125*, 3194.

(10) Knoth, W. H.; Domaille, P. J.; Harlow, R. L. *Inorg. Chem.* **1986**, *25*, 1577.

(11) Bi, L.-H.; Kortz, U.; Nellutla, S.; Stowe, A. C.; van Tol, J.; Dalal, N. S.; Keita, B.; Nadjo, L. *Inorg. Chem.* **2005**, *44*, 896.

(12) Wassermann, K.; Palm, R.; Lunk, H. J.; Fuchs, J.; Steinfeldt, N.; Stösser, R. *Inorg. Chem.* **1995**, *34*, 5029.

(13) (a) Muller, A.; Peters, F.; Pope, M. T.; Gatteschi, D. *Chem. Rev.* **1998**, 240. (b) Clemente-Juan, J. M.; Coronado, E. *Coord. Chem. Rev.* **1999**, *193–195*, 361.

(14) See, for example, the recent special issue on POMs in *J. Mol. Catal. A: Chem.* **2007**, *262*, 1.

(15) (a) Zhang, S.-T.; Yuan, D.-Q.; Zhang, J.; Yang, G.-Y. *Inorg. Chem.* **2007**, *46*, 4569. (b) Zheng, S.-T.; Yuan, D.-Q.; Jia, H.-P.; Zhang, J.; Yang, G.-Y. *Chem. Commun.* **2007**, 1858.

two-dimensional (2D) structures.[16] On another hand, the functionalization of transition metal substituted POMs by organic ligands remains largely unexplored. The acetato ligand is the most often encountered,[17] probably because syntheses of POMs are often carried out in acetate buffer, but examples of a chiral POM incorporating zirconium ions bound to tartrate ligands[18] and of a dimeric dititanium substituted polyoxotungstate with oxalate ligands[19] have also been recently reported. Besides, the synthesis of $[PW_{11}O_{39}Co(pbpy)]^{5-}$ (pbpy = 5-phenyl-2-(4-pyridinyl)pyridine)[20] indicates that hydrothermal conditions can induce the replacement of water molecules coordinated to transition metal ions encapsulated within POMs by organonitrogen ligands, but the report of the structures of imidazole[21] and pyridine[22] coordinated sandwich type compounds $[\{Co(C_3H_4N_2)\}_3(B\text{-}\alpha\text{-}BiW_9O_{33})_2]^{12-}$ and $[\{Ni(C_5H_5N)\}_3(B\text{-}\alpha\text{-}AsW_9O_{33})_2]^{12-}$ shows that functionalized sandwich type POMs can also be prepared under mild conditions.

For several years, our group has been exploring the functionalization of POMs, mainly by azido and carboxylato groups, using usual bench conditions. This has allowed us to isolate macromolecular complexes as well as 1D to three-dimensional (3D) materials.[23] In parallel we have studied the reactivity of vacant POMs under hydrothermal conditions, in the presence of transition metal ions and amines, considering first the reaction of Fe^{III} ions with PW_{11}[24] and PW_9[25] units. The present study combines these two approaches and reports on the reactivity of $Fe_4(H_2O)_{10}Sb_2W_{18}$,[6] prepared in situ, toward organic ligand (oxalate, ethylenediamine) both under hydrothermal conditions and at room temperature. This precursor was chosen because of the ten accessible water molecules on the iron centers (Figure 1b) which are potentially exchangeable by organic ligands. Four novel compounds based on trivacant polyoxotungstates binding iron centers are described, leading to a comparison between conventional synthetic methods and hydrothermal conditions for the substitution of water molecules on the iron centers embedded into the POM structures and the obtaining of 0D or 1D frameworks. The magnetic properties of one of these compounds, a mixed-valent hexanuclear iron complex, are also reported.

Experimental Section

Synthesis. $Na_9[\alpha\text{-}SbW_9O_{33}]\cdot 19.5H_2O$ was synthesized according to a published procedure.[26] The hydrothermal syntheses were carried out in polytetrafluoroethylene lined stainless steel containers under autogenous pressure. The 23 mL vessel was filled to approximatively 25% volume capacity (Vi ~ 6 mL). All reactants were stirred briefly before heating. The samples were heated to 130 °C for **1** and **3** or 160 °C for **4** over a period of 4 h, kept at 130 or 160 °C for 40 h, and cooled to room temperature over a period of 44 h. The mixture pH was measured before (and noted pH_i) and after the reaction (and noted pH_f). The products were isolated by filtration and washed with ethanol.

Preparation of $[enH_2]_3[Fe_4(H_2O)_8(SbW_9O_{33})_2]\cdot 20H_2O$ (1). A mixture of $Na_9[\alpha\text{-}SbW_9O_{34}]\cdot 19.5H_2O$ (0.200 g, 0.0697 mmol), $FeCl_3$ (0.096 g, 0.355 mmol), en (300 μL, 4.2 mmol), and H_2O (5 mL) was stirred, and the pH was adjusted to 2.5 (pH_i) with 4 M HCl (pH_f = 1.8). Yellow crystals (0.039 g, yield 21% based on W) were collected by filtration. IR (KBr pellets, ν/ cm^{-1}, Supporting Information Figure S1): 1612 (s), 1504 (s), 1325 (w), 1037 (w), 955 (s), 868 (sh), 793 (s), 750 (sh), 631 (m), 516 (w), 472 (w), 426 (w), 354 (m). Anal. Calcd for **1**: C, 1.30; H, 1.57; N, 1.52; Fe, 4.04; W, 59.92. Found: C, 1.43; H, 1.28; N, 1.55; Fe, 3.96; W, 59.30.

Preparation of $[dapH_2]_3[Fe_4(H_2O)_8(SbW_9O_{33})_2]\cdot 20H_2O$ (dap = 1,3-diaminopropane) (1b). A mixture of $Na_9[\alpha\text{-}SbW_9O_{34}]\cdot 19.5H_2O$ (0.200 g, 0.0697 mmol), $FeCl_3$ (0.096 g, 0.355 mmol), dap (300 μL, 4.2 mmol), and H_2O (5 mL) was stirred, and the pH was adjusted to 2.0 (pH_i) with 4 M HCl (pH_f = 1.0). Yellow crystals (0.054 g, yield 21% based on W) were collected by filtration. IR: 1607 (s), 1495 (m), 1463 (m), 1185 (w), 952 (s), 881 (sh), 776 (s), 639 (m), 512 (w), 473 (w), 418 (w), 354 (m). Anal. Calcd for **1b**: C, 1.94; H, 1.67; N, 1.51; Fe, 4.01; W, 59.46. Found: C, 2.24; H, 1.55; N, 1.25; Fe, 3.89; W, 59.77.

Preparation of $Na_{14}[Fe_4(C_2O_4)_4(H_2O)_2(SbW_9O_{33})_2]\cdot 60H_2O$ (2). A solution of $[Fe_4(H_2O)_{10}(\beta\text{-}SbW_9O_{33})_2]^{6-}$ ($Fe_4(H_2O)_{10}Sb_2W_{18}$) was synthesized according to the procedure described by Kortz et al.[6] starting from 4 g (1.6 mmol) of $Na_9[\alpha\text{-}SbW_9O_{34}]\cdot 19.5H_2O$. To this solution was added $H_2C_2O_4$ (0.800 g, 8.89 mmol). The pH was adjusted to 3.0 by addition of 2 M NaOH. The solution progressively lightened while stirring at room temperature for 1 h. Slow evaporation at room temperature led to yellow crystals which were collected by filtration and dried in air (0.960 g, yield 18% based on W). IR (KBr pellets, ν/ cm^{-1}, Supporting Information Figure S1): 1666 (s), 1504 (m), 1415 (m), 1317 (w), 1271 (w), 1173 (w), 1037 (w), 940 (s), 865 (sh), 785 (s), 757 (sh), 649 (m), 516 (w), 462 (w), 426 (w), 354 (m). Anal. Calcd for **2**: C, 1.45; H, 1.89; Na, 4.86; Fe, 3.37; W, 49.96. Found: C, 1.62; H, 1.15; Na, 4.73; Fe, 3.39; W, 49.97.

Preparation of $[enH_2]_7[Fe_4(C_2O_4)_4(SbW_9O_{33})_2]\cdot 14H_2O$ (3). A mixture of $Na_9[\alpha\text{-}SbW_9O_{34}]\cdot 19.5H_2O$ (0.200 g, 0.0697 mmol), $FeCl_3$ (0.096 g, 0.355 mmol), $H_2C_2O_4$ (0.040 g, 0.444 mmol), en (450 μL, 5.6 mmol), and H_2O (5 mL) was stirred, and the pH was adjusted to 6.0 (pH_i) with 4 M HCl (pH_f = 4.5). Yellow crystals (0.076 g, yield 37% based on W) were collected by filtration. IR (KBr pellets, ν/ cm^{-1}, Supporting Information Figure S1): 1656 (s), 1628 (s), 1422 (m), 1278 (m), 947 (s), 873 (sh), 793 (s), 767 (sh), 657 (m), 516 (w), 470 (w), 344 (w). Anal. Calcd for **3**: C, 4.50; H, 1.68; N, 3.34; Fe, 3.80; W, 56.36. Found: C, 4.66; H, 1.71; N, 3.56; Fe, 3.63; W, 56.60.

(16) (a) Wang, J.-P.; Du, X.-D.; Niu, J.-Y. *Chem. Lett.* **2006**, *35*, 1408. (b) Zheng, S.-T.; Wang, M.-H.; Yang, G.-Y. *Chem. Asian J.* **2007**, *2*, 1380.

(17) (a) Wassermann, K.; Lunk, H.-J.; Palm, R.; Fuchs, J.; Steinfeldt, N.; Stösser, R.; Pope, M. T. *Inorg. Chem.* **1996**, *35*, 3273. (b) Kortz, U. *J. Cluster Sci.* **2003**, *14*, 205. (c) Mialane, P.; Dolbecq, A.; Rivière, E.; Marrot, J.; Sécheresse, F. *Eur. J. Inorg. Chem.* **2004**, 33.

(18) Fang, X.; Anderson, T. M.; Hill, C. L. *Angew. Chem., Int. Ed.* **2005**, *44*, 3540.

(19) Hayashi, K.; Murakami, H.; Nomiya, K. *Inorg. Chem.* **2006**, *45*, 8078.

(20) Han, Z.; Zhao, Y.; Peng, J.; Ma, H.; Liu, Q.; Wang, E. *J. Mol. Struct.* **2005**, *738*, 1.

(21) Wang, H. L.; Xue, G. L.; Wang, J. W.; Wang, D. Q.; Li, J.; Shi, Q. Z. *Acta Chim. Sin.* **2003**, *61*, 1839.

(22) Liu, X.-M.; Wang, C.-R.; Liu, B.; Xue, G.-L.; Hu, H.-M.; Wang, J.-W.; Fu, F. *Chin. J. Chem.* **2005**, *23*, 1412.

(23) Mialane, P.; Dolbecq, A.; Sécheresse, F. *Chem. Commun.* **2006**, 3477.

(24) Pichon, C.; Dolbecq, A.; Mialane, P.; Marrot, J.; Rivière, E.; Goral, M.; Zynek, M.; McCormac, T.; Borshch, S. A.; Zueva, E.; Sécheresse, F. *Chem.—Eur. J.* [Online early access]. DOI: 10.1002/chem.200700896. Published Online: 2008. http://dx.doi.org/10.1002/chem.200700896.

(25) Pichon, C.; Dolbecq, A.; Mialane, P.; Marrot, J.; Rivière, E.; Sécheresse, F. *Dalton Trans.* **2008**, 71.

(26) Bösing, M.; Loose, I.; Pohlmann, H.; Krebs, B. *Chem.—Eur. J.* **1997**, *3*, 1232.

Table 1. Crystallographic Data for **1**–**4**

	1	2	3	4
empirical formula	$C_6H_{86}Fe_4N_6O_{94}Sb_2W_{18}$	$C_8H_{124}Fe_4Na_{14}O_{144}Sb_2W_{18}$	$C_{22}H_{98}Fe_4N_{14}O_{96}Sb_2W_{18}$	$C_{14}H_{116}Fe_6N_{14}O_{92}W_{18}$
formula weight, g	5523.01	6622.98	5871.34	5597.61
crystal system	triclinic	triclinic	triclinic	monoclinic
space group	$P\bar{1}$	$P\bar{1}$	$P\bar{1}$	$P2_1/n$
a/Å	17.9519(9)	12.5898(15)	13.0759(4)	16.640(5)
b/Å	21.6279(11)	14.9339(17)	13.9123(5)	12.125(4)
c/Å	22.9122(12)	19.739(2)	15.3954(5)	22.066(7)
α/deg	111.673(2)	111.350(5)	95.957(2)	90
β/deg	104.041(2)	101.661(6)	114.2990(10)	109.343(7)
γ/deg	92.192(2)	93.977(6)	105.570(2)	90
V/Å^3	7939.0(7)	3343.4(7)	2834.56(14)	4201(2)
Z	4	1	1	2
T/K	293	220	293	293
ρ_{calc}/g cm^{-3}	4.621	3.152	4.089	4.425
μ/mm^{-1}	27.474	16.393	22.885	25.673
data/parameters	46293/2227	19483/801	13966/770	12202/595
R_{int}	0.0337	0.0810	0.0490	0.0632
GOF	1.321	1.190	1.224	1.013
R ($>2\sigma(I)$)	$R_1 = 0.0284$ $wR_2 = 0.0745$	$R_1 = 0.0450$ $wR_2 = 0.1247$	$R_1 = 0.0421$ $wR_2 = 0.1236$	$R_1 = 0.0462$ $wR_2 = 0.0959$

$^aR_1 = (\sum||F_o| - |F_c||)/\sum|F_c|$. $^bwR_2 = (\sum w(F_o^2 - F_c^2)^2/\sum w(F_o^2)^2)^{1/2}$.

Preparation of $[enH_2]_5[Fe_4(enH)_2(FeW_9O_{34})_2]\cdot 24H_2O$ (4). A mixture of $Na_9[\alpha\text{-}SbW_9O_{34}]\cdot 19.5H_2O$ (0.200 g, 0.0697 mmol), $FeCl_3$ (0.096 g, 0.355 mmol), en (450 μL, 5.6 mmol), and H_2O (5 mL) was stirred, and the pH was adjusted to 7.0 (pH_i) with 4 M HCl ($pH_f = 6.8$). Brown crystals (0.050 g, yield 26% based on W) were collected by filtration. IR (KBr pellets, ν/ cm^{-1}, Supporting Information Figure S1): 1612 (m), 1504 (m), 1325 (w), 1088 (w), 1035 (w), 937 (s), 847 (s), 767 (sh), 714 (s), 613 (m), 524 (w), 434 (w), 380 (w), 362 (w), 326 (w), 300 (w). Anal. Calcd for **4**: C, 3.00; H, 2.09; N, 3.50; Fe, 5.99; W, 59.12. Found: C, 2.94; H, 1.63; N, 3.11; Fe, 6.38; W, 59.10.

X-ray Crystallography. Intensity data collections were carried out with a Bruker Nonius X8 APEX 2 diffractometer for all the structures except for **4** for which the data were collected with a Siemens SMART three-circle diffractometer, each equipped with a CCD bidimensional detector using the monochromatized wavelength λ(Mo Kα) = 0.71073 Å. The absorption correction was based on multiple and symmetry-equivalent reflections in the data set using the SADABS program[27] based on the method of Blessing.[28] The structures were solved by direct methods and refined by full-matrix least-squares using the SHELX-TL package.[29] In all the structures there is a discrepancy between the formulas determined by elemental analysis and the formulas deduced from the crystallographic atom list because of the difficulty in locating all the disordered water molecules, a common feature among the structures of polyoxotungstates.[30] The data set for **2** which has the largest "voids" was corrected with the program SQUEEZE, a part of the PLATON package of crystallographic software used to calculate the solvent disorder area and to remove its contribution to the overall intensity data.[31] As crystals of **2** rapidly loose water at room temperature, a crystal was glued in Paraton-N oil, and the data set collected at 220 K. In the structure of **3** there is a disorder on one of the trimetallic W_3O_{13} groups; a disorder scheme (Supporting Information Figure S4) with two positions labeled A (with occupancy factor 0.8) and B (with occupancy factor 0.2) is proposed. Crystallographic data are given in Table 1. Selected bond distances are listed in Table 2.

Elemental Analysis. Elemental analyses were performed by the Service Central d'Analyze Elémentaire, CNRS, 69360 Solaize, France.

Infrared Spectra. IR spectra were recorded on an IRFT Magna 550 Nicolet spectrophotometer using the technique of pressed KBr pellets.

Thermogravimetric Analysis (TGA) Measurements. Thermogravimetry was carried out under N_2/O_2 (1:1) flow (60 mL min^{-1}) with a Perkin-Elmer electrobalance TGA-7 at a heating rate of 10 °C min^{-1} up to 800 °C.

Magnetic Measurements. Magnetic susceptibility measurements were carried out with a Quantum Design SQUID Magnetometer with an applied field of 1000 G using powder samples pressed in pellets to avoid preferential orientation of the crystallites. The independence of the susceptibility value with regard to the applied field was checked at room temperature. The susceptibility data were corrected from the diamagnetic contributions as deduced by using Pascal's constant tables.

Results and Discussion

Syntheses, IR Spectroscopy, and X-ray Powder Diffraction. We have explored the reactivity of $[\alpha\text{-}SbW_9O_{33}]^{9-}$ toward Fe^{III} ions under various conditions, summarized in Figure 2. While under conventional conditions, this trivacant anion has been widely studied, to our knowledge there is only one compound isolated under hydrothermal conditions which contains this POM and Cu^{II} ions.[32] Kortz et al. have shown that the reaction of $[\alpha\text{-}SbW_9O_{33}]^{9-}$ with Fe^{III} in an acidic solution heated at 90 °C leads to the formation of the dimeric $Fe_4(H_2O)_{10}Sb_2W_{18}$ anion (Figure 1b).[6] When the same reaction mixture is heated at 130 °C under hydrothermal conditions in the presence of ethylenediamine (en) a

(27) Sheldrick, G. M. *SADABS; program for scaling and correction of area detector data*; University of Göttingen: Germany, 1997.
(28) Blessing, R. *Acta Crystallogr.* **1995**, *A51*, 33.
(29) Sheldrick, G. M. *SHELX-TL, Software Package for the Crystal Structure Determination*, version 5.03; Siemens Analytical X-ray Instrument Division: Madison, WI, U.S.A., 1994.
(30) (a) Sadakane, M.; Dickman, M. H.; Pope, M. T. *Angew. Chem., Int. Ed.* **2000**, *39*, 2914. (b) Zhang, C.; Howell, R. C.; Scotland, K. B.; Perez, F. G.; Torado, L.; Francesconi, L. C. *Inorg. Chem.* **2004**, *43*, 7691. (c) Zhang, Z.; Qi, Y.; Qin, C.; Li, Y.; Wang, E.; Wang, X.; Su, Z.; Xu, L. *Inorg. Chem.* **2007**, *46*, 8162. (d) Belai, N.; Pope, M. T. *Chem. Commun.* **2005**, *46*, 5760.
(31) van der Sluis, P.; Spek, A. L. *Acta Crystallogr., Sect. A.* **1990**, *46*, 194.
(32) Wang, J.; Ma, P.; Li, J.; Niu, J. *Chem. Lett.* **2006**, *35*, 994.

Table 2. Selected Bond Lengths (Å) and Valence Bond Summations (Σ_s) for Compound **1**–**4** Associated to the Representations Of Supporting Information Figures S3−S5.

Compound 1					
Fe(1)−O(8)	1.935(4)	$\Sigma_s = 3.16$	Fe(5)−O(86)	1.945(4)	$\Sigma_s = 3.12$
Fe(1)−O(20)	1.948(4)		Fe(5)−O(99)	1.946(4)	
Fe(1)−O(31)	1.953(4)		Fe(5)−O(74)	1.948(4)	
Fe(1)−O(32)	1.978(3)		Fe(5)−O(98)	1.974(3)	
Fe(1)−O(133)	2.080(4)		Fe(5)−O(141)	2.109(4)	
Fe(1)−O(134)	2.126(4)		Fe(5)−O(142)	2.134(4)	
Fe(2)−O(12)	1.925(3)	$\Sigma_s = 3.03$	Fe(6)−O(78)	1.936(3)	$\Sigma_s = 3.05$
Fe(2)−O(23)	1.963(3)		Fe(6)−O(90)	1.956(3)	
Fe(2)−O(33)	1.974(4)		Fe(6)−O(97)	1.980(4)	
Fe(2)−O(56)	2.008(4)		Fe(6)−O(122)	2.038(4)	
Fe(2)−O(135)	2.102(4)		Fe(6)−O(143)	2.064(4)	
Fe(2)−O(136)	2.148(4)		Fe(6)−O(144)	2.117(5)	
Fe(3)−O(57)	1.957(3)	$\Sigma_s = 2.96$	Fe(7)−O(111)	1.939(3)	$\Sigma_s = 3.07$
Fe(3)−O(45)	1.962(3)		Fe(7)−O(123)	1.944(3)	
Fe(3)−O(64)	1.986(4)		Fe(7)−O(130)	1.961(3)	
Fe(3)−O(24)	2.030(4)		Fe(7)−O(89)	2.019(4)	
Fe(3)−O(137)	2.069(4)		Fe(7)−O(145)	2.075(5)	
Fe(3)−O(138)	2.159(4)		Fe(7)−O(146)	2.153(4)	
Fe(4)−O(41)	1.928(4)	$\Sigma_s = 3.13$	Fe(8)−O(107)	1.939(4)	$\Sigma_s = 3.14$
Fe(4)−O(53)	1.938(4)		Fe(8)−O(132)	1.947(3)	
Fe(4)−O(66)	1.953(4)		Fe(8)−O(131)	1.955(4)	
Fe(4)−O(65)	1.963(3)		Fe(8)−O(119)	1.960(4)	
Fe(4)−O(139)	2.110(4)		Fe(8)−O(148)	2.118(4)	
Fe(4)−O(140)	2.172(4)		Fe(8)−O(147)	2.122(4)	
Compound 2					
Fe(1)−O(2)	1.951(6)	$\Sigma_s = 3.19$	Fe(2)−O(26)	1.942(6)	$\Sigma_s = 3.03$
Fe(1)−O(15)	1.960(6)		Fe(2)−O(23)	1.960(6)	
Fe(1)−O(33)	1.965(6)		Fe(2)−O(1)	1.986(6)	
Fe(1)−O(3)	1.974(6)		Fe(2)−O(36)	2.045(6)	
Fe(1)−O(34)	2.050(6)		Fe(2)−O(37)	2.047(7)	
Fe(1)−O(35)	2.076(6)		Fe(2)−O(38)	2.123(6)	
Compound 3					
Fe(1)−O(32)	1.976(4)	$\Sigma_s = 3.06$	Fe(2)−O(2)	1.968(4)	$\Sigma_s = 2.70$
Fe(1)−O(8)	1.979(3)		Fe(2)−O(31A)	2.007(3)	
Fe(1)−O(33)	1.979(5)		Fe(2)−O(20)	2.042(4)	
Fe(1)−O(23)	1.984(3)		Fe(2)−O(38)	2.059(4)	
Fe(1)−O(34)	2.057(4)		Fe(2)−O(39)	2.092(5)	
Fe(1)−O(35)	2.091(5)		Fe(2)−O(1)	2.205(4)	
Compound 4					
Fe(1)−O(34)	1.826(8)	$\Sigma_s = 3.11$	Fe(3)−O(33)	2.087(9)	$\Sigma_s = 1.95$
Fe(1)−O(18)	1.847(8)		Fe(3)−O(8)	2.117(9)	
Fe(1)−O(12)	1.867(8)		Fe(3)−O(27)	2.152(8)	
Fe(1)−O(6)	1.869(8)		Fe(3)−O(34)	2.160(8)	
Fe(2)−O(14)	1.979(9)	$\Sigma_s = 2.91$	Fe(3)−O(20)	2.188(8)	
Fe(2)−O(29)	1.990(9)		Fe(3)−N(2A)	2.212(11)	
Fe(2)−O(34)	2.026(8)				
Fe(2)−O(34)	2.036(8)				
Fe(2)−O(27)	2.062(8)				
Fe(2)−O(20)	2.081(8)				

condensation reaction is observed, leading to $[enH_2]_3[Fe_4(H_2O)_8(SbW_9O_{33})_2]\cdot 20H_2O$ (**1**). **1** is an insoluble 1D compound resulting from the elimination of two water molecules on the two external iron centers of the $Fe_4(H_2O)_{10}Sb_2W_{18}$ precursor and contains enH_2^{2+} counterions. $Na_{14}[Fe_4(ox)_4(H_2O)_2(SbW_9O_{33})_2]\cdot 60H_2O$ (**2**) is the sodium salt of the discrete $[Fe_4(ox)_4(H_2O)_2(SbW_9O_{33})_2]^{14-}$ anion, noted $Fe_4ox_4(H_2O)_2Sb_2W_{18}$, and is obtained in a moderate yield by the reaction at room temperature of $Fe_4(H_2O)_{10}Sb_2W_{18}$ with an excess of oxalic acid added directly in the synthetic mixture at pH < 3. As observed for **1**, heating this solution at 130 °C under hydrothermal conditions leads to the condensation of the functionalized $Fe_4ox_4(H_2O)_2Sb_2W_{18}$ anion and the formation of 1D chains in $[enH_2]_7[Fe_4(C_2O_4)_4(SbW_9O_{33})_2]\cdot 14H_2O$ (**3**). When the heating temperature is raised to 160 °C, the POM precursor decomposes, and Fe^{III} iron centers substitute Sb^{III} ions as heteroelements to form

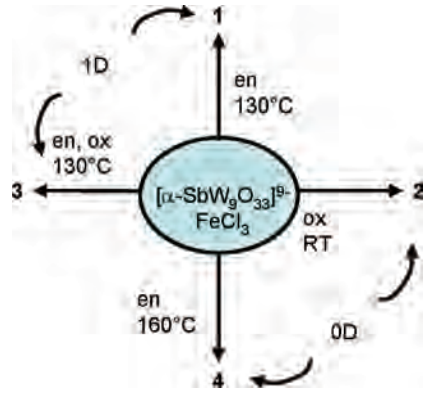

Figure 2. Scheme summarizing the experimental conditions for the synthesis of **1**–**4**.

$[enH_2]_5[Fe_4(enH)_2(FeW_9O_{34})_2]\cdot 24H_2O$ (**4**) which contains isolated sandwich type $\{Fe^{II}_2{>}Fe^{III}_2(enH)_2(Fe^{III}W_9O_{34})_2\}$ POMs where two monoprotonated ethylenediamine ligands have replaced the two external water molecules of the well-known rhombohedral Fe_4O_6 core. Furthermore, these two external iron centers have been reduced. It is well known that amines create reducing atmospheres under hydrothermal conditions,[33] primary amines working as better reducing agents than secondary and tertiary amines. However, and quite surprisingly, when non reducing reactants such as tetramethylammonium (TMA) ions are introduced as counterions the $\{Fe^{III}_4(H_2O)_2(Fe^{III}W_9O_{34})_2\}$ POM does not form. Instead, beige crystals of the TMA salt of the Keggin type anion $(TMA)_5Fe^{III}W_{12}O_{40}\cdot nH_2O$ are isolated.[34] As usually observed, the formation of **1**, **3**, and **4** under hydrothermal conditions is also highly dependent on the synthetic parameters such as pH, temperature, and proportion of reactants. For example, **1** only forms in the pH domain 2.5–3.5. At pH > 6 crystalline powders of **4** are isolated, even at 130 °C. The presence of en is not essential for the condensation reaction but necessary for its crystallization, and the analogous product **1b** with 1,3-diaminopropane has been isolated. Crystals of **3** are only obtained for 6 < pH < 7 and for [ox]/[SbW_9] ratios lower than 6.5 at 130 °C but can equally be synthesized at 160 °C, suggesting that oxalate ligands stabilize the $Fe_4ox_4(H_2O)_2Sb_2W_{18}$ POM. Considering **4**, we have attempted to rationalize the synthetic procedure by using a Fe^{II} precursor (with $[Fe^{II}]/[Fe^{III}] = 1:2$) or by starting from Na_2WO_4 instead of SbW_9 as the source of W. Although the products have similar IR spectra and X-ray powder diffraction patterns, only the synthesis using SbW_9 leads to a compound with a satisfactory elemental analysis. Finally, **1**, **3**, and **4** can be synthesized starting from the sodium salt of the $Fe_4(H_2O)_{10}Sb_2W_{18}$ precursor,[6] but the crystallinity of the products is improved by the one step procedure.

(33) (a) See for example: Pasha, I.; Choudhury, A.; Rao, C. N. R. *Inorg. Chem.* **2003**, *42*, 409. (b) Wang, X.-L.; Qin, C.; Wang, E.-B.; Su, Z. M.; Li, Y.-G.; Xu, L. *Angew. Chem., Int. Ed.* **2006**, *45*, 7411. (c) Xu, Y.; Nie, L.-B.; Zhu, D.; Song, Y.; Zhou, G. P.; You, W.-S. *Cryst. Growth Des.* **2007**, *5*, 925.

(34) $a = 13.361(3)$, $b = 20.997(5)$, $c = 45.558(9)$ Å, $\alpha = \beta = \gamma = 90°$, $V = 12781(8)$ Å^3.

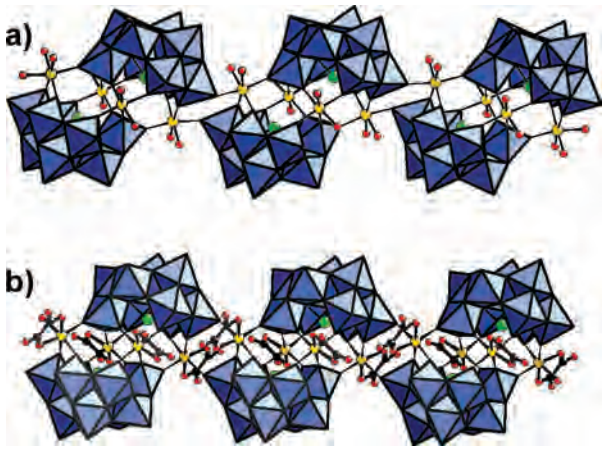

Figure 3. (a) View of the 1D chain running along the [01$\bar{1}$] axis in **1**; (b) view of the 1D chain running along the [100] axis in **3**; blue octahedra, WO_6; green spheres, Sb; yellow spheres, Fe; red spheres, O.

The infrared spectra of **1**−**3** are similar in the 400–1000 cm^{-1} region (Supporting Information Figure S1), which is indicative of the W═O and W−O−Fe vibrations of the POM, and are also close to the IR spectrum of $Fe_4(H_2O)_{10}Sb_2W_{18}$ with a resolution intermediate between that of the sodium salt[6] and that of the tetrahexylammonium salts.[35] As expected, because of a change in the structure of the POM, the IR spectrum of **4** is different (Supporting Information Figure S1), especially in the 400–800 cm^{-1} region. The peaks characteristics of the organic molecules are present in the 1100–1700 cm^{-1} region. The peaks of the oxalato ligand (marked with stars) can be identified in **2** and **3,** and the peaks of the protonated enH_2^{2+} ions (marked with diamonds) are easily detected in **1**, **2**, and **4**. On a side note, the position, as well as the number of bands observed, for the oxalato group in this region is consistent with its coordination mode as a bidentate ligand and can be compared, for instance, to the bands observed in the $[Mo_2S_2O_2(C_2O_4)_2(H_2O)_2]^{2-}$[36] or $[Mo_2O_4(H_2O)_2(C_2O_4)_2]^{2-}$[37] anions.

A comparison of the experimental X-ray diffraction powder patterns of the four compounds and of the powder patterns calculated from the structure solved from single crystal X-ray diffraction data confirms the bulk compositions.

Structures. The structure of **1** can be viewed as the stacking of 1D anionic chains running along the [0 1 −1] axis with diprotonated ethylenediamine counterions located around the chains. The chain (Figure 3a) results from the elimination of two water molecules on the outer iron centers of a $Fe_4(H_2O)_{10}Sb_2W_{18}$ anion (Figure 1b) and the concomitant formation of Fe−O−W bonds with two adjacent POMs. The anion in **2** (Figure 4a) also directly derives from $Fe_4(H_2O)_{10}Sb_2W_{18}$ and results from the substitution of two water molecules on each iron center by one oxalato ligand. The anionic charge of the POM increases and is balanced by the presence of 14 sodium counter-ions, four of which

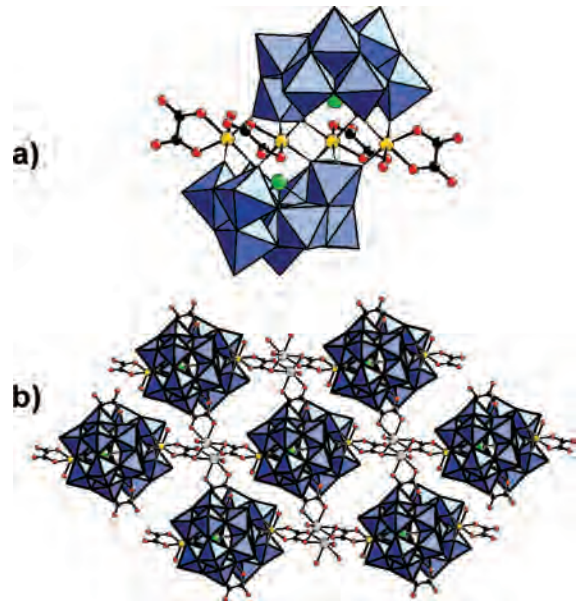

Figure 4. (a) Mixed polyhedral and ball and stick representation of the functionalized dimeric POM in **2**; (b) view of the plane formed by the connection of the dimeric POMs by sodium counter-ions in **2**; blue octahedra, WO_6; green spheres, Sb; yellow spheres, Fe; red spheres, O; grey spheres, Na.

playing a particular role. These four cations are bound to the oxygen atoms of three oxalato ligands of three different functionalized anions and induce the formation of a layered structure (Figure 4b). The structure of **3** (Figure 3b) can be considered as resulting either from the functionalization of the 1D chain of **1** (Figure 3a) by oxalato ligands (one oxalato ligand substituting the two labile water molecules still present on each iron center) or from the condensation of the functionalized POMs of **2**. The condensation process and/or the functionalization by oxalato ligands only induce small changes on the geometrical parameters within the $Fe_4(H_2O)_{10}Sb_2W_{18}$ POM (Supporting Information Figure S3, Table 2). In all cases the iron atoms are in an octahedral environment, the total number of water molecules on the four atoms decreasing from 10 to 0 from $Fe_4(H_2O)_{10}Sb_2W_{18}$ to **3**. Valence bond calculations[38] (Table 2) confirm that all the iron ions have a +III oxidation state in **1**−**3**.

The POM in **4** has the well-known sandwich type structure with two $[B\text{-}\alpha\text{-}FeW_9O_{34}]^{11-}$ anions encapsulating a tetranuclear iron cluster. Compared to the classical sandwich type POMs three differences can be noticed: (i) the heteroelement is not Si^{IV}, Ge^{IV}, P^{V}, or As^{V} as usually observed but an Fe^{III} ion in a tetrahedral environment, as in the parent $[Fe^{III}_4(H_2O)_2(Fe^{III}W_9O_{34})_2]^{10-}$ anion reported by Krebs et al.;[39] (ii) the tetranuclear iron cluster is a mixed-valence cluster; and (iii) the two water molecules on the two external iron centers have been substituted by nitrogen atoms of monoprotonated ethylenediamine cations. The mixed-valence state has been determined by bound valence sum calculations (Table 2) and confirmed by elemental analysis and the magnetic study (see below). The two external iron centers

(35) Bonchio, M.; Carraro, M.; Farinazzo, A.; Sartorel, A.; Scorrano, G.; Kortz, U. *J. Mol. Catal. A: Chem.* **2007**, *262*, 36.
(36) du Peloux, C.; Dolbecq, A.; Cadot, E.; Marrot, J.; Sécheresse, F. *J. Mol. Struct.* **2003**, *656*, 37.
(37) Mialane, P.; Dolbecq, A.; Costaz, G.; Lisnard, L.; Marrot, J.; Sécheresse, F. *Inorg. Chem. Commun.* **2002**, *5*, 702.
(38) Blessing, R. *Acta Crystallogr.* **1995**, *A51*, 33.
(39) Limanski, E. M.; Piepenbrink, M.; Droste, E.; Burgemeister, K.; Krebs, B. *J. Cluster Sci.* **2002**, *13*, 369.

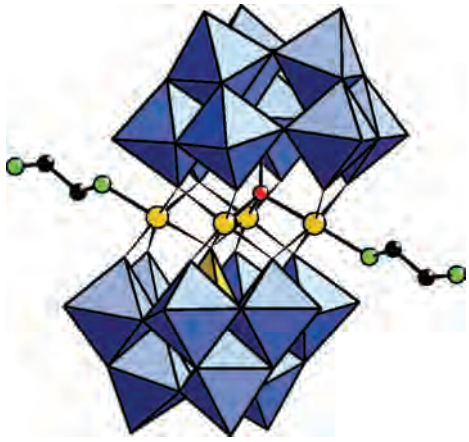

Figure 5. Sandwich type POM in **4**; blue octahedra, WO_6; yellow octahedra, Fe; black spheres, C; light green spheres, N.

are Fe^{II} ions while the four remaining ones are Fe^{III} centers, in agreement with a recent theoretical study which shows that in $[Fe^{III}_4(H_2O)_2(PW_9O_{34})_2]^{6-}$ the first reduction occurs at the external Fe atoms coordinated to a water ligand.[40] Examples of sandwich type POMs encapsulating Cu^{II},[41] Ni^{II}[16b] tetranuclear cluster ions bound to organonitrogen ligands have been recently reported, with pending or bridging ethylenediamine ligands. Despite several attempts, syntheses at higher initial pH values have not led to the deprotonation of the pending enH ligand and the formation of a 1D chain. The free ethylenediamine counterions are diprotonated. The NH_3^+ groups of the pending ligands are hydrogen bonded with short distances to oxygen atoms of the POM (Supporting Information Figure S6).

Magnetic Properties. As in the clusters **1**, **2**, and **3**, the embedded paramagnetic centers only weakly interact; the nature of the magnetic exchange interactions and of the ground-state have been investigated only for compound **4**. The magnetization vs *B*/*T* has been recorded at 2, 4, and 6 K (Figure 5; Figure 6, inset). The experimental curves indicate that **4** possesses an $S = 5$ ground state, a situation which has been found in several hexanuclear iron clusters.[42] A fit of the data considering the zero field splitting (ZFS) Hamiltonian $\hat{H} = g_u\beta\hat{S}_uH + D[\hat{S}_z^2 - \hat{S}(\hat{S}+1)/3] + E(\hat{S}_x^2 - \hat{S}_y^2)$ where $u = x, y, z$ and D and E are the axial and rhombic ZFS parameters, respectively, affords $D = +1.12$ cm^{-1}, $E/D = 0.15$, and $g = 2.046$ ($R = 4.7 \times 10^{-5}$).[43] The unambiguous determination of the sign of D requires measurements on a single crystal or high field EPR studies.[44] However, in the present case, only a positive value of D gives satisfactory fits of the $M = f(B/T)$ curves (Supporting Information Figure S7). Compared to previously reported iron systems, the determined D value is large for an $S = 5$ state,[45] confirming that POM ligands induce very large magnetic anisotropy as previously evidenced in Mn^{II} POM clusters.[46]

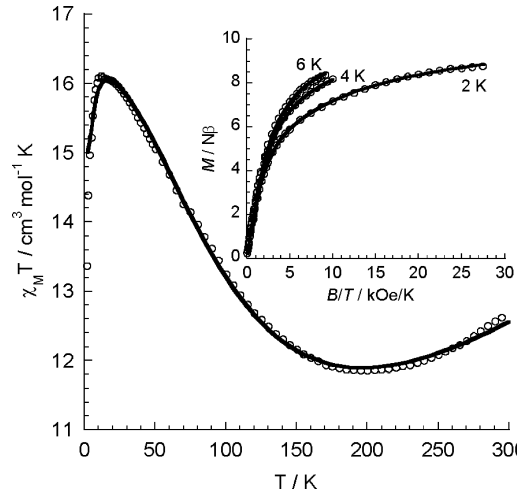

Figure 6. Thermal dependence of $\chi_M T$ for **4**. Inset: magnetization vs magnetic field divided by temperature at 2, 4, and 6 K from right to left; the solid lines represent the best fitting results (see text).

The $\chi_M T = f(T)$ curve related to **4** is reported in Figure 6. The $\chi_M T$ product at room temperature (12.6 cm^3 mol^{-1} K) is lower than the calculated $\chi_M T$ value of 24.7 cm^3 mol^{-1} K for four high spin Fe^{III} and two high spin Fe^{II} non interacting centers (assuming $g = 2.05$), confirming that the iron centers are magnetically interacting in **4**. Three domains must be distinguished in the $\chi_M T = f(T)$ curve. First, the $\chi_M T$ product decreases from 300 to 200 K ($\chi_M T = 11.8$ cm^3 mol^{-1} K). Then, $\chi_M T$ increases until $T = 16$ K ($\chi_M T = 16.0$ cm^3 mol^{-1} K). Such behavior can be due to the concomitant presence of ferromagnetic and antiferromagnetic interactions, and/or to spin frustration phenomena,[47] which must occur in **4** considering the topology of the system. Finally, the $\chi_M T$ curve rapidly decreases from 10 to 2 K ($\chi_M T = 13.4$ cm^3 mol^{-1} K). This is most likely due to the large ZFS of the ground-state and to the weak intramolecular antiferromagnetic interactions between nondirectly bound metal centers as negligible intermolecular antiferromagnetic interactions are expected considering the long Fe···Fe intermolecular distances in **4** ($d_{Fe\cdots Fe} > 8.90$ Å). Taking into account the topology of complex **4**, four exchange parameters must be considered (Figure 7a) as no acceptable simplified model can be envisaged. The Hamiltonian related to compound **4** can thus be expressed as

$$\hat{H} = -J_1(\hat{S}_{Fe1a}\hat{S}_{Fe2a} + \hat{S}_{Fe1a}\hat{S}_{Fe2b} + \hat{S}_{Fe1b}\hat{S}_{Fe2a} + \hat{S}_{Fe1b}\hat{S}_{Fe2b}) - J_2(\hat{S}_{Fe1a}\hat{S}_{Fe3a} + \hat{S}_{Fe1b}\hat{S}_{Fe3b}) - J_3(\hat{S}_{Fe2a}\hat{S}_{Fe3a} + \hat{S}_{Fe2a}\hat{S}_{Fe3b} + \hat{S}_{Fe2b}\hat{S}_{Fe3a} + \hat{S}_{Fe2b}\hat{S}_{Fe3b}) - J_4(\hat{S}_{Fe2a}\hat{S}_{Fe2b})$$

with $\hat{S}_{Fe1a} = \hat{S}_{Fe1b} = \hat{S}_{Fe2a} = \hat{S}_{Fe2b} = 5/2$ and $\hat{S}_{Fe3a} = \hat{S}_{Fe3b} =$

(40) Romo, S.; Fernández, J. A.; Maestre, J. M.; Keita, B.; Nadjo, L.; de Graaf, C.; Poblet, J. M. *Inorg. Chem.* **2007**, *46*, 4022.
(41) Fan, L.; Wang, Li, Y.; An, H.; Xiao, D.; Wang, X. *J. Mol. Struct.* **2007**, *841*, 28.
(42) Cañada-Vilalta, C.; O'Brien, T. A.; Brechin, E. K.; Pink, M.; Davidson, E. R.; Christou, G. *Inorg. Chem.* **2004**, *43*, 5505.
(43) $R = [\Sigma(M_{calc} - M_{obs})^2/\Sigma(M_{obs})^2]$.
(44) Chen, W.-Z.; Cotton, A.; Dalal, N. S.; Murillo, C. A.; Ramsey, C. M.; Ren, T.; Wang, X. *J. Am. Chem. Soc.* **2005**, *127*, 12691.
(45) Accorsi, S.; Barra, A.-L.; Caneschi, A.; Chastanet, G.; Cornia, A.; Fabretti, A. C.; Gatteschi, D.; Moetalò, C.; Olivieri, E.; Parenti, F.; Rosa, P.; Sessoli, R.; Sorace, L.; Wernsdorfer, W.; Zobbi, L. *J. Am. Chem. Soc.* **2006**, *128*, 4742.
(46) Pichon, C.; Mialane, P.; Rivière, E.; Blain, G.; Dolbecq, A.; Marrot, J.; Sécheresse, F.; Duboc, C. *Inorg. Chem.* **2007**, *46*, 7710.
(47) Mc Kusker, J. K.; Vincent, J. B.; Schmitt, E. A.; Mino, M. L.; Shin, K.; Cokin, D. K.; Hagen, P. M.; Huffman, J. C.; Chrisyou, G.; Hendrickson, D. N. *J. Am. Chem. Soc.* **1991**, *113*, 3012.

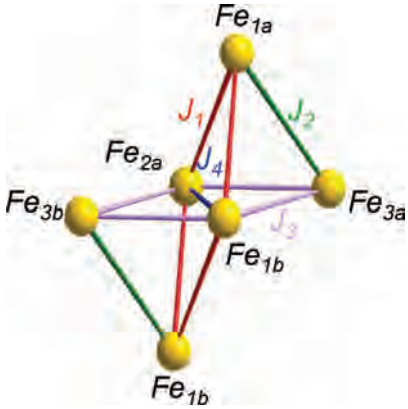

Figure 7. Coupling scheme for compound **4**.

2. The best fit of the experimental $\chi_M T$ data in the 300−10 K temperature range assuming a single g value of 2.046 for the six iron centers gave $J_1 = +7.0$ cm^{-1}, $J_2 = -95.6.0$ cm^{-1}, $J_3 = -21.8$ cm^{-1}, and $J_4 = -22.9$ cm^{-1} ($R = 2.2 \times 10^{-4}$).[48] The positive value of the weakest coupling constant J_1 must be considered with care as it is well-known that $Fe^{III}-O(X)-Fe^{III}$ systems are antiferromagnetically coupled,[49] but no satisfactory fit with four negative exchange parameters could be found. The energy diagram derived from these values confirm the presence of an $S = 5$ ground state, with a first excited-state $S = 6$ located at 9.5 cm^{-1}.

To the best of our knowledge, there are no hexanuclear {Fe_6} complexes relevant to complex **4** for which both the structural and the magnetic data have been reported. Nevertheless, Nair and Hagen have characterized the [$Fe_6(\mu_4$-$O)_2(\mu_2$-$OMe)_8(OMe)_4(tren)_2]^{2+}$ cation (tren = 2,2′,2″-triaminotriethylamine) noted here Fe_6tren_2,[50] which possesses an {Fe_6} core arranged in a fashion similar to **4**. These two complexes can be compared, even if Fe_6tren_2 contains six Fe^{III} centers in an octahedral environment and the six O(W) bridging groups constituting **4** are replaced by six alkoxo ligands in Fe_6tren_2. Interestingly, it has been found that Fe_6tren_2 also possesses an $S = 5$ ground state, suggesting that the oxidation state of the external Fe_{3a} and Fe_{3b} centers has no influence on the nature of the ground state. Finally, even if the electronic parameters have not been quantified for the complex Fe_6tren_2, the study of the $M = f(B/T)$ curves clearly shows that the magnetic anisotropy of the $S = 5$ state in **4** is much larger than in Fe_6tren_2.

Conclusions

To conclude, this study highlights the possibility of functionalizing transition metal substituted POMs by organic ligands at room temperature or under hydrothermal conditions. Elimination of two water molecules of the $Fe_4(H_2O)_{10}Sb_2W_{18}$ POM has led to a 1D insoluble chain (**1**) with ethylenediamine counter-ions. With oxalato ligands, hydrothermal conditions have favored the formation of a 1D compound (**3**) while a molecular complex (**2**) has been isolated at room temperature. When the precursor has been heated at 160 °C, a sandwich type POM (**4**) with a hexanuclear mixed-valence Fe cluster has been obtained. The magnetic study shows that this complex possesses an $S = 5$ ground-state with a large magnetic anisotropy. The three insoluble compounds **1**, **3**, and **4** are promising candidates for applications in heterogeneous catalysis while the reactivity of the soluble $Fe_4(ox)_4(H_2O)_2Sb_2W_{18}$ POM (**2**) with transition metal cations, which could substitute the sodium ions bound to the terminal positions of the oxalato ligands, will lead to heterobimetallic compounds particularly appealing in the field of magnetism. Finally, another extension of this work could be the use under hydrothermal conditions of protonated bulky amines in place of ethylenediamine to study the cation effect on the formation of POMs. Indeed, this strategy has been largely explored under conventional synthetic conditions and has highlighted that the choice of the amino counterion plays a crucial role on the nature of the obtained POM.[51] A similar effect could be expected under hydrothermal conditions.

Supporting Information Available: X-ray crystallographic CIF data in PDF format for **1**–**4**, and Figures S1−S7 of infrared spectra, thermogravimetric analysis, partial atomic labeling scheme of **1**, **2**, **3**, **4**, and so forth (PDF). This material is available free of charge via the Internet at http://pubs.acs.org.

IC7024186

(48) $R = [\Sigma(\chi_M T_{calc} - \chi_M T_{obs})^2/\Sigma(\chi_M T_{obs})^2]$.
(49) Kurtz, D. M. *Chem. Rev.* **1990**, *90*, 585.
(50) Nair, V. S.; Hagen, K. S. *Inorg. Chem.* **1992**, *31*, 4048.
(51) (a) Ritchie, C.; Burkholder, E. M.; Long, D.-L.; Adam, D.; Kögerler, P.; Cronin, L. *Chem. Commun.* **2007**, 468. (b) Long, D.-L.; Burkholder, E.; Cronin, L. *Chem. Soc. Rev.* **2007**, *36*, 105. and references therein.